EFDA–JET–PR(12)58

M.N.A. Beurskens, L. Frassinetti, C. Challis, C. Giroud, S. Saarelma, B. Alper, C. Angioni, P. Bilkova, C. Bourdelle, S. Brezinsek, P. Buratti, G. Calabro, T. Eich, J. Flanagan, E. Giovannozzi, M. Groth, J. Hobirk, E. Joffrin, M.J. Leyland, P. Lomas, E. de la Luna, M. Kempenaars, G. Maddison, C. Maggi, P. Mantica, M. Maslov, G. Matthews, M-L. Mayoral, R. Neu, I. Nunes, T. Osborne, F. Rimini, R. Scannell, E.R. Solano, P.B. Snyder, I. Voitsekhovitch, P. de Vries and JET EFDA contributors

Global and Pedestal Confinement in JET with a Metallic Wall

Global and Pedestal Confinement in JET with a Metallic Wall

M.N.A. Beurskens[1], L. Frassinetti[2], C. Challis[1], C. Giroud[1], S. Saarelma[1], B. Alper[1], C. Angioni[3], P. Bilkova[4], C. Bourdelle[5], S. Brezinsek[6], P. Buratti[7], G Calabro[7], T. Eich[3], J. Flanagan[1], E. Giovannozzi[7], M. Groth[8], J. Hobirk[3], E. Joffrin[5], M.J. Leyland[9], P. Lomas[1], E. de la Luna[10], M. Kempenaars[1], G. Maddison[1], C. Maggi[3], P. Mantica[11], M. Maslov[1], G. Matthews[1], M-L. Mayoral[1], R. Neu[3], I. Nunes[12], T. Osborne[13], F. Rimini[1], R. Scannell[1], E.R. Solano[11], P.B. Snyder[13], I. Voitsekhovitch[1], P. de Vries[14] and JET EFDA contributors*

JET-EFDA, Culham Science Centre, OX14 3DB, Abingdon, UK

[1]EURATOM-CCFE Fusion Association, Culham Science Centre, OX14 3DB, Abingdon, OXON, UK
[2]Division of Fusion Plasma Physics, Association EURATOM-VR, KTH, SE-10044 Stockholm, Sweden
[3]Max-Planck-Institut für Plasmaphysik, EURATOM Association, D-85748 Garching, Germany
[4]EURATOM/IPP ASCR-Association Prague, Czech republic
[5]Association Euratom-CEA, IRFM, F-13108 St-Paul-Lez-Durance, France
[6]Association EURATOM/Forschungszentrum Juelich GmbH 52425 Juelich Germany
[7]Associazione EURATOM-ENEA sulla Fusione, C.R. Frascati, Frascati, Italy
[8]Association EURATOM/AaltoUniversity 02015 Espoo Finland
[9]Department of Physics, University of York, Heslington, York, YO10 5DD, UK
[10]Laboratorio Nacional de Fusion, Asociacion EURATOM-CIEMAT, Madrid, Spain
[11]Istituto di Fisica del Plasma 'P.Caldirola', Associazione EURATOM-ENEA-CNR, Milano, Italy
[12]Instituto de Plasmas e Fusão Nuclear, Associação EURATOM-IST, Lisboa, Portugal
[13]General Atomics, PO Box 85608, San Diego, California 92186-5608, USA
[14]Association EURATOM/DIFFER, Rijnhuizen P.O. Box 1207 3430BE Nieuwegein, Netherlands
** See annex of F. Romanelli et al, "Overview of JET Results", (24th IAEA Fusion Energy Conference, San Diego, USA (2012)).*

Preprint of Paper to be submitted for publication in
Nuclear Fusion

ABSTRACT

Type I ELMy H-mode operation in JET with the ITER like Be/W wall (JET-ILW) generally occurs at lower pedestal pressures compared to those with the full carbon wall (JET-C). The pedestal density is similar but the pedestal temperature where Type I ELMs occur is reduced and below to the so-called critical Type I-Type III transition temperature reported in JET-C experiments. Furthermore, the confinement factor $H_{98(y,2)}$ in Type I ELMy H-mode baseline plasmas is generally lower in JET-ILW compared to JET-C at low power fractions $P_{net}/P_{thr,08} < 2$ (where P_{net} is the net input power, and $P_{thr,08}$ the L-H power threshold from [Martin-JPCS-2008]). Higher power fractions have thus far not been achieved in the baseline plasmas. At $P_{net}/P_{thr,08} > 2$, the confinement in JET-ILW hybrid plasmas is similar to that in JET-C. A reduction in pedestal pressure is the main reason for the reduced confinement in JET-ILW baseline ELMy H-mode plasmas where typically $H_{98(y,2)} = 0.8$ is obtained, compared to $H_{98(y,2)} = 1.0$ in JET-C. In JET-ILW hybrid plasmas a similarly reduced pedestal pressure is compensated by an increased peaking of the core pressure profile resulting in $H_{98(y,2)} \leq 1.25$. The pedestal stability has significantly changed in high triangularity baseline plasmas where the confinement loss is also most apparent. Applying the same stability analysis for JET-C and JET-ILW, the measured pedestal in JET-ILW is stable with respect to the calculated Peeling Ballooning stability limit and the ELM collapse time has increased to 2ms from typically 200ms in JET-C. This indicates that changes in the pedestal stability may have contributed to the reduced pedestal confinement in JET-ILW plasmas. A comparison of EPED1 pedestal pressure prediction with JET-ILW experimental data in over 500 JET-C and JET-ILW baseline and hybrid plasmas shows a good agreement with $0.8 < (\text{measured } p_{ped}) / (\text{predicted } p_{ped,EPED}) < 1.2$, but that the role of triangularity is generally weaker in the JET-ILW experimental data than in the model predictions

1. INTRODUCTION.

The reference operational scenario for ITER is the type-I ELMy H-mode plasma. Based on a large data set from many tokamaks worldwide, a reference inductive scenario (scenario 2 in [IPB-NF-2007]) has been defined with a plasma current of $I_p = 15$MA at a toroidal field of $B_t = 5.3$T and $q_{95} = 3$ from which the primary goal of ITER to achieve operation at $Q_{DT} = P_{fus}/P_{input} = 10$ can be projected with some confidence. The plasma confinement factor, based on the scaling from the 1998 ITER Physics Basis (IPB98) study [IPB-NF-1999], required for this so-called 'baseline ELMy H-mode' scenario is $H_{98(y,2)} = 1$ at a normalised pressure of $\beta_N = 1.8$ and a Greenwald density fraction of $n/n_{gw} = 0.85$. Furthermore, an averaged plasma triangularity of $\delta_{av} = 0.45$ is required. The latter requirement is not obtained from the IPB98 scaling but stems from dedicated experiments in current tokamaks showing the beneficial effects of plasma triangularity on both energy and particle confinement in JET [Saibene-NF-1999] and other tokamaks [Kamada-IAEA-1996, Osborne-PPCF-2000, Stober-PPCF-2000]. A second scenario is considered for ITER at reduced current I_p=12MA, and increased bootstrap current with ~50% non-inductive current

drive, leading to operation at elevated $H_{98(y,2)}$ = 1-1.2 and increased β_N = 2-2.5. This so-called hybrid scenario (scenario 3 in [IPB-NF-2007]) compensates lower plasma current operation by improved energy confinement in order to achieve Q_{DT} = 6.

Both baseline ELMy H-mode and hybrid plasma scenarios have been successfully achieved in JET with the carbon wall (JET-C). For the JET baseline plasmas the study of 1) the low triangularity shape [e.g. Nunes-IAEA-2010] was conducted to obtain low density and a low collisionality approaching that expected in ITER. 2) The high triangularity baseline studies were aimed at achieving an ITER relevant shape as well as operation at the densities associated with high triangularity operation [Saibene-PPCF-2002, Giroud-NF-2012, Beurskens-NF-2013, Leyland-NF-submitted]. These studies have shown that the ITER requirements of $H_{98(y,2)}$=1 at a normalised pressure of β_N = 1.8 and a Greenwald density fraction of n/n_{gw}=0.85 is achievable in high triangularity plasmas in JET with the carbon wall.

The JET-C hybrid studies were aimed at 1) in low triangularity hybrid plasmas; establishing maximum benefit of q-profile shaping to obtain low magnetic shear in conditions of high rotational shear and low plasma density and hence with poor equipartition between ion and electron stored energies. [Joffrin-IAEA-2010, Hobirk-PPCF-2012]. Under these conditions enhanced ion profile peaking is observed benefiting the energy confinement [Beurskens-NF-2013], 2) in high triangularity hybrid plasmas: obtaining a strong pedestal through shaping and high b_N operation and via profile stiffness an enhancement in the core stored energy [Beurskens-NF-2013]. The high triangularity hybrid scenario is less sensitive to q-profile tailoring with respect to core confinement enhancement, but the scenario does benefit from low shear operation to avoid the occurrence of confinement degrading MHD modes in the plasma core [Joffrin-IAEA-2010]. Both low and high triangularity JET-C hybrid plasmas have well exceeded the ITER performance requirements and have achieved $H_{98(y,2)}$ = 1.4 at $\beta_N \leq 3.5$ [Joffrin-IAEA-2010, Hobirk-PPCF-2012]. Although both low and high triangularity hybrid scenarios have offered good plasmas performance, the high triangularity hybrid scenario is thought to be more viable for ITER where a strong coupling of ions and electrons is expected due to high density operation [Beurskens-NF-2013].

Operation in ITER with a Deuterium Tritium fuel mix is envisaged with a Be main chamber wall and W divertor instead of a fully carbon plasma facing wall. The main reason for the choice of a metal first-wall in ITER is to achieve a significant reduction in long-term tritium retention [Hawryluk-NF-2009, Brezinsek-PSI-2012, Matthews-PSI-2012]. In preparation for ITER, the main plasma facing components of JET-C have been replaced with a new ITER-like wall (JET-ILW), with mostly Be in the main chamber and W in the divertor. Experiments in JET-ILW can for the first time test the influence of the planned ITER wall material mix on plasma performance. Experience in ASDEX Upgrade [Kallenbach-NF-2011, Schweinzer-NF-2011], with a full W wall, and Alcator C-mod [Lipschultz-PoP-2006], with a full Molybdenum wall, shows that it is to be expected that the plasma operational space is reduced due to the necessity to minimise high-Z impurity influxes and hence will require increased plasma density operation. In addition, a study has been conducted

comparing the impact of metal walls on baseline ELMy H-mode confinement in ASDEX Upgrade and JET [Beurskens-PPCF-2013]. Secondly the capacity to deal with steady-state and transient heat loads is reduced with a Be/W wall composition compared to the fully C wall, which will require enhanced divertor radiation which is facilitated through increased density operation.

This paper will evaluate the impact of the Be/W wall on global confinement as well as the separate changes in the pedestal and core contributions to confinement. The paper will first show an example of operation in Type I ELMy H-mode plasmas in JET-ILW at a lower pedestal pressure compared to JET-C. This indicates that already from this observation the pedestal confinement and hence global confinement has changed. Secondly The global confinement in JET-C and JET-ILW baseline ELMy H-mode and hybrid plasmas is studied and related to the applied input power compared to the L-H threshold power, power degradation of the confinement and the scaling of normalised confinement with normalised pressure β_N. Next the local changes in the temperature and density profiles is studied and the core and pedestal contribution to the confinement is compared, showing that both core transport as well as the pedestal confinement may has changed in JET-ILW compared to JET-C. The pedestal stability is further studied in a comparison of a typical ELMy H-mode baseline plasma from JET-C and JET-ILW, where the change in confinement is most apparent at high triangularity. Finally a global comparison with the predictive pedestal code EPED is presented.

2. ACCESS TO TYPE I ELMY H-MODE WITH C AND BE/W WALL.

In order to illustrate the change in accessible operational regime an example is shown of two similar plasmas in JET-C and JET-ILW where a gas ramp was applied. During the gas ramp both plasmas undergo a transition from Type I to Type III ELMy H-mode at constant input power [Huber-PSI-2012]. The plasmas presented have a toroidal field of B_T=3T, plasma current of I_p=2 MA and an input power of P_{net}=10MW for JET-C and B_T=2.9T, I_p=2 MA and P_{net}=8MW for JET-ILW for a high triangularity (δ=0.4) plasma configuration. Figure 1 shows time traces for these plasmas and shows that as the fuelling is increased, the plasma density increases and the H-mode confinement is degraded, while the ELM type changes from regular type I ELMs to more frequent type III ELMs and eventually transits to L-mode for the JET-ILW plasma.

Hyperbolic tangent fits to individual High Resolution Thomson Scattering (HRTS) pedestal profiles [Pasqualotto-RSI-2004, Frassinetti-RSI-2012] are used to monitor the pedestal electron density (n_e) and temperature (T_e) evolution. Figure 2 shows the pedestal T_e-n_e diagram for both the JET-C and JET-ILW plasmas for multiple profile-fits during the gas-ramps. For both plasmas the pedestal density increases while the pedestal temperature decreases during the gas ramp such that the temporal evolution of the two discharges move from the top left to the bottom right in Figure 2. The figure shows that the pedestal pressure degrades (see the comparison with the isobars in Figure 2) while it cools down. For JET-C a transition from Type I to high frequency Type III ELMs occurs at a pedestal temperature of $T_{e,ped} \approx 650$eV. In JET-ILW a transition from Type I ELMs to a type III ELMs is observed at a much lower temperature $T_{e,ped} \approx 280$eV. This change of over a factor

of two in $T_{e,ped}$ at the transition cannot be explained by critical temperature model for the Type I to Type III transition [Igitkhanov-CPB-2000, Sartori-PPCF-2004 and Giroud-NF-2012]. This model has no power dependence and would expect only a $B_T^{10/17}$ or at most a B_T^2 dependence, whereas the magnetic fields of the JET-C and JET-ILW plasmas are similar.

Note that although the Type I ELM regime can be accessed at lower pedestal temperature for JET-ILW, this does not provide a confinement benefit, See also [Giroud-IAEA-2013]. In JET-ILW the type I ELM regime is accessed at a lower normalised confinement $H_{98(y,2)}$. This example illustrates that changes in the pedestal stability may have occurred in JET-ILW, which then have affected the global confinement as well.

3. CONFINEMENT OF TYPE I ELMY H-MODE PLASMAS IN JET-C AND JET-ILW

In JET-ILW both the baseline and the hybrid Type I ELMy H-mode plasma scenarios have been (re-)established at low and high plasma triangularity [Joffrin-IAEA-2010, Joffrin-IAEA-2012]. A confinement database for these scenarios containing 115 baseline H-mode and hybrid plasmas in the JET-C is described in [Frassinetti-EPS-2010, Beurskens-NF-2013]. A new JET-ILW scenario confinement database has been constructed with over 400 baseline H-mode and hybrid plasmas. An overview of the covered triangularity, safety factor (q_{95}) and plasmas currents are given in Table 1. Only plasmas identified as Type I ELMy H-modes have been included in the database. Generally the plasma configurations have been kept similar between the JET-C and JET-ILW scenario development. Unfortunately, due to constrains on the divertor geometry in JET-ILW the low triangularity hybrid experiments had to be conducted at an somewhat increased triangularity ($0.2 \rightarrow 0.25$) compared to the JET-C experiment as indicated in table 1.

Each of the scenarios are described in detail in [Joffrin-IAEA-2010, Joffrin-IAEA-2012]; The baseline ELMy H-mode plasmas typically operate with $\beta_N \leq 2$ and have $q_{95} = 2.8\text{-}3.6$. They do not feature any deliberate current profile pre-shaping, and have a late onset of the additional heating. The hybrid plasmas have $q_{95} = 3.5\text{-}4.5$ and feature early heating and a current overshoot before the heating phase in order to shape the current profile to avoid large sawtooth activity and, at least temporarily, avoid the generation of confinement compromising m/n = 3/2 and 4/3 NTM activity [Hobirk-PPCF-2012]. Thanks to the high input power and low plasma current in these plasmas, high values of normalized pressure can be achieved up to $\beta_N \leq 3.5$.

The database study presented here includes hybrid and baseline plasmas that form a typical cross section for the JET-C and JET-ILW campaigns. The experimental aims in the development of each of the scenarios were to establish plasmas with an optimal plasma performance. This has moved scenario developers to particular choices in plasma configuration and particular choice of fuelling level and heating schemes. In the JET-C experiments the database is representative of the best performance plasmas in either of the scenarios, whereas in the JET-ILW experiments the scenario development is still on-going and the database represents the current state of development. It is aimed at in upcoming experiments to further optimise the plasma performance in JET-ILW.

Operation with the Be/W wall has lead to a narrower access to stable plasma operation, where higher fuelling levels than in the carbon wall experiments are required [Joffrin-IAEA-2012, Pueterich-IAEA-2012]. Although JET-C reference plasmas were prepared for comparative studies with JET-ILW, high performance was optimised with low gas fuelling in some JET-C scenarios, limiting the database overlap. Figure 3 shows the confinement factor $H_{98(y,2)}$ for all four scenarios as a function of gas fuelling. In JET-C, baseline ELMy H-mode plasmas achieved good normalised confinement with $H_{98(y,2)} \approx 1$ in un-fuelled plasmas (Figure 3a and 3b). High triangularity baseline plasmas could be fuelled up to the Greenwald density without loss of normalised confinement, where also a transition in ELM regime was observed from pure Type I to mixed Type I/II ELMs at the high densities (Figure 4a) and [Saibene-PPCF-2002, Giroud-NF-2012, Leyland-NF-submitted]. On the contrary the JET-ILW high triangularity base line plasmas show a reduced normalised confinement by 10-30% across the entire fuelling scan compared to the JET-C plasmas [Giroud-IAEA-2012]. No change in ELM regime from pure Type I to mixed Type I/II was observed at high density in the JET-ILW experiments. The change in confinement in these high triangularity pulses is unlikely due to a change in plasma radiation. In the absence of carbon as a radiator, the divertor radiation is reduced in JET-ILW compared to JET-C [Giroud-IAEA-2012, Joffrin-IAEA-2012], and in the absence of strong W contamination, the core radiation in JET-ILW is similar or even a bit lower than in JET-C. The low triangularity baseline plasmas in the JET-C database where only operated at low gas-fuelling in order to optimise their performance [Nunes-IAEA-2010]. As in the JET-ILW experiments increased fuelling was required to avoid W contamination there is insufficient overlap at the higher gas fuelling levels for the JET-C and JET-ILW low triangularity baseline data. However in previous JET-C studies [e.g. Saibene-PPCF-2002] a clear degradation of the plasma confinement with gas fuelling was observed in low triangularity plasmas. Unfortunately these pulses could not be used for the study presented here due their lack of pedestal data. Nevertheless Figure 3b) suggests that the difference in normalised confinement as a function of gas fuelling is less prominent for the low triangularity plasmas than it was for the high triangularity plasma in Figure 3a). Figure 4 gives corroborating evidence; in JET-C the plasma normalised confinement was shown to reduce with increasing Greenwald density fraction n_e/n_{gw} [Saibene-NF-1999, Saibene-PPCF-2002], and increased plasmas triangularity would improve the normalised confinement for a given n_e/n_{gw}. Figure 4a shows that indeed this is again found for the JET-C database presented here. Figure 4b shows that the low triangularity JET-ILW plasmas follow this trend well and the confinement is degraded with n_e/n_{gw} following the low triangularity trend of the JET-C database. However, the high triangularity baseline plasmas lay well below the data trend for high triangularity baseline plasmas in JET-C, supporting the suggestion that these plasmas have undergone a further confinement reduction compared to the JET-C experiments.

The global normalised confinement of the hybrid plasmas in JET-ILW is comparable to that in JET-C for both low and high triangularity hybrid plasmas. In JET-C the achievable confinement was best at low or zero gas fuelling, where $H_{98(y,2)} \leq 1.4$ was achieved for both low and high

triangularity. In JET-ILW this was not achievable due to the need to mitigate W accumulation with gas fuelling [Joffrin-IAEA-2012, Pueterich-IAEA-2012]. However at similar fuelling levels the confinement in low and high triangularity hybrid plasmas was at par in the JET-ILW experiments compared to the JET-C experiments and $H_{98(y,2)} = 1.2\text{-}1.3$ was achieved. Important for the remaining study in this paper is that JET-ILW experiments covered a range of input powers from $P_{NBI} = 11\text{-}23$MW for the high triangularity and $P_{NBI} = 3\text{-}24$MW for the low triangularity hybrid plasmas, for similar fuelling levels in the range of $0.5\text{-}1.5\times10^{22}$ electrons/s.

In summary, to avoid W contamination JET-ILW plasmas require increased gas fuelling, which has contributed to a reduced plasma energy confinement. However the confinement in JET-C and JET-ILW plasmas is generally the same when a similar gas fuelling level is applied, Figure 3. The only large deviation to this observation is found in the high triangularity baseline plasmas. These plasmas generally show a degraded confinement in JET-ILW compared to JET-C for all fuelling levels.

The normalised confinement of the JET-C and JET-ILW plasmas is compared to the proximity to the L-H transition power threshold as in [Sartori-PPCF-2004]. For the comparison the net input power $P_{NET} = (P_{in}–dW/dt)$ is compared to the threshold power from the international scaling $P_{thr,08}$ in [Martin-JPCS-2008]. Figure 5 shows that JET-C baseline ELMy H-mode plasmas could achieve good normalised confinement with $H_{98(y,2)} \approx 1$ at low power levels above the threshold $P_{NET}/P_{thr,08} = 1.2\text{-}2.5$. However for the baseline ELMy H-mode plasmas, the achieved normalised confinement is reduced for JET-ILW compared to JET-C for the range of input powers covered here: $P_{NET}/P_{thr,08} = 1.2\text{-}2.5$. As a comparison, the hybrid plasmas in this study cover the range $P_{NET}/P_{thr,08} \leq 4.5$. There is no apparent difference between the JET-C and JET-ILW hybrid experiments in achieved normalised confinement for a given $P_{NET}/P_{thr,08} = 2.5–4.5$. A (weak) connection is made between the hybrid and baseline plasmas for the low input power hybrid plasmas. Figure 5b shows that also for the hybrid plasmas the normalised confinement is reduced to $H_{98(y,2)} < 1$ for $P_{NET}/P_{thr,08} \leq 2.5$. With the neutral beam power upgrade in 2013 from 25MW to 35MW it can be studied whether the baseline ELMy H-mode confinement can be recovered at elevated $P_{NET}/P_{thr,08}$.

The scaling of confinement with input power is studied in Figure 6 showing the energy confinement time τ_e normalised to the IPB-98 [IPB-NF-1999] scaling excluding the power scaling as $\tau_e/(0.0562\times I_p^{0.93} B_t^{0.15} n_e^{0.41} R^{1.39} k^{0.78} a^{0.58} M^{0.19})$. In JET-C the hybrid and baseline plasmas are off-set as the baseline plasmas feature a lower $H_{98(y,2)}$ than the hybrid plasmas, but both scenarios follow a similar power degradation consistent with the t_{98} scaling of $P^{-0.69}$. Figure 6b shows that the JET-ILW baseline ELMy H-mode plasmas are consistent with the same scaling of $P^{-0.69}$ but lie on a lower confinement "branch" compared to JET-C plasmas. The Hybrid plasmas cut across from the lower JET-ILW baseline confinement branch for the low input power hybrid plasmas to the higher JET-C confinement branch for the higher input power hybrid plasmas. For illustration purposes the dashed line in Figure 6b follows data where $I_p < 2.1$MA.

The latter indicates that normalised pressure rather than absolute input power may be driving the

normalised confinement improvement. Indeed Figure 7 shows that a very strong correlation exists between β_N and $H_{98(y,2)}$. Within the existence diagram of Figure 7 good normalised confinement is only achieved at elevated b_N. The new JET-C and JET-ILW datasets corroborate earlier findings that the b-degradation of confinement in the IPB-98 scaling as $\tau_e \sim \beta_{th}^{0.9}$ is too strong [Luce-PPCF-2008]. In fact a linear regression to the current data-set shows that $H_{98(y,2)} \sim \beta_{th}^{0.81\pm0.02}$ and hence the β dependence of the confinement time as good as disappears in this global JET-C/JET-ILW database. As stated in [McDonald-NF-2007] an absence of the β degradation in the energy confinement scaling suggests that operation at elevated b_N is beneficial for the fusion gain at high β_N.

4. PEDESTAL CONTRIBUTION TO CONFINEMENT

The pedestal confinement is characterised using hyperbolic tangent fits to the electron temperature and density from combined HRTS profiles in a steady time window of minimum 1s and maximum 5s duration, depending on the selected discharge stationarity. Ion temperature profiles from Charge Exchange Recombination Spectroscopy (CXRS) are unfortunately not available for the entire JET-ILW database. For the baseline plasmas we can safely assume $T_i = T_e$ as the energy exchange time between ions and electrons is small compared to the energy confinement time, however for the hybrids we need to bear in mind that possibly $T_i > T_e$ as was seen in JET-C [Beurskens-NF-2013]. The electron pedestal densities, $n_{e,ped}$ and temperatures $T_{e,ped}$ from HRTS are shown in Figure 8. As I_p varies in the database a normalisation to the plasma current is performed by comparing the Greenwald density fraction $n_{e,ped}/n_{gw}$ ($\sim n_{e,ped}/I_p$) with T_{ped}/I_p to enable a comparison of the data along curves of constant pedestal poloidal pressure $b_{pol,ped}$ (which scales as $1/I_p^2$). As a comparison the relation of the thermal stored energy W_{th}, normalised to I_p and B_t following the $IPB_{98,y2}$ scaling, and input power is shown as well in Figure 8.

A first observation is that most JET-ILW plasma scenarios have a lower maximum achieved $T_{e,ped}$ compared to their JET-C counterpart, which is at least not completely compensated by an increase in $n_{e,ped}$. Hence the pedestal confinement is reduced for the ILW plasmas. Figure 8a shows that the largest loss in pedestal pressure is found in the high triangularity baseline plasmas. The pedestal pressure in JET-ILW high triangularity baseline plasmas is lost through a reduction of the pedestal temperature by 20-30% compared to the JET-C plasmas, as was reported in [Giroud-IAEA-2012]. For a similar or even increased range of input powers in JET-ILW the achieved pedestal pressure is lower in JET-ILW compared to JET-C for all scenarios. Arguably, the highest pedestal pressure in the low triangularity hybrid plasmas is similar to that achieved in JET-C, but in JET-ILW that was achieved at ~20% higher input power compared to JET-C low triangularity hybrid plasmas, Figure 8h.

Figures 9a and 9b show the coupling of the total poloidal normalised pressure b_p and the thermal electron pedestal pressure from HRTS (total = both thermal and non-thermal components obtained from diamagnetic loop measurements). As discussed in [Beurskens-NF-2013] in JET-C a coupling between the total and pedestal poloidal pressure β_p and $\beta_{p,ped}$ is observed as expected from edge

linear MHD stability theory [e.g. Snyder-NF-2007]. In addition, for the JET-C plasmas in Figure 9a a clear separation occurs between the low and high triangularity plasmas, which is again expected from edge stability theory; increasing triangularity improves the edge stability and can lead to increased pedestal confinement. However, for JET-ILW the beneficial effect of triangularity has disappeared and low and high triangularity baseline and hybrid plasmas both coincide with the low triangularity plasmas in JET-C, as is seen in Figure 9b. So increasing the triangularity seems not to be beneficial for edge stability in JET-ILW, neither for baseline plasmas nor for the hybrid plasmas. A strong co-linearity, linked to core profile stiffness, is observed between the total thermal $\beta_{p,thermal}$ and pedestal $\beta_{p,ped}$ for both JET-C and JET-ILW, as can be seen in Figure 9c and 9d. This indicates that the total thermal confinement is set by the pedestal stored energy combined with a strong degree of core profile stiffness for the thermal core profiles. A small deviation occurs between the JET-ILW and JET-C hybrid plasmas in Figure 9d, indicating a variation in the core confinement contribution between the two datasets, as will be discussed in section 5.

5. CORE CONTRIBUTION TO CONFINEMENT

The role of the core confinement is studied by comparing the T_e and n_e profile shapes. The so-called peakedness of the profiles is studied (defined as the ratio of the profile values at a radius $\rho_{tor} \sim 0.4$ and at $\rho_{tor} \sim 0.8$), using JET HRTS data. The ion temperature profiles from Charge Exchange recombination spectroscopy are not yet available for the ILW-database.

For JET-C, a strong degree of pressure profile peaking conservation was observed across the scenarios Figure 10a & 10c and [Beurskens-NF-2013]. This is caused by a flattening of the density profile, and a steepening of the temperature profiles with increasing effective collisionality n_{eff} ($n_{eff} = 1 \cdot 10^{14} \cdot R_{geo} \cdot z_{eff} \cdot \langle n_e \rangle / \langle T_e \rangle^2$, where $\langle n_e \rangle$ and $\langle T_e \rangle$ are volume averaged, and R_{geo} is the geometrically averaged major radius).

For JET-ILW, the trend in density peaking with collisionality is well reproduced, Figure 10b. However the density peaking at low collisionality is no longer compensated by a flattening of the temperature profile, and the pressure peaking is no longer conserved, Figure 10d. Figure 10b shows that whereas the baseline plasmas feature a similar peaking of T_e and n_e for both JET-C and JET-ILW, the confinement contribution due to core temperature profile peaking is enhanced for the hybrid plasmas in JET-ILW compared to JET-C hybrid plasmas.

6. PEDESTAL STABILITY AND COMPARISON WITH MODELLING

In general in JET-ILW plasmas the pedestal confinement has decreased compared to JET-C plasmas with similar input parameters. One important driver is the required increased fuelling level, which apparently has a cooling effect on the pedestal. In addition the effect of shaping, i.e. triangularity, which used to help improving the pedestal stability and hence the global confinement in JET-C through profile stiffness, seems to have disappeared. The plasmas most affected are the high triangularity baseline plasmas, but also the high triangularity hybrid plasmas are affected.

In the latter the confinement loss is not as apparent, as the core confinement is increased due to increased profile peaking. To start the investigation of the edge stability we here first concentrate on the high triangularity baseline plasmas and then study the other scenarios in a wider modelling comparison using the EPED code.

For the high triangularity baseline plasmas the ILW experiment has given access to Type I ELMy H-mode operation in a low confinement state with $H_{98(y,2)} \approx 0.8$, previously the domain of Type III ELMy H-mode in JET-C [Sartori-PPCF-2004]. The ELMs have been classified as Type I following the simple rule that f_{ELM} increases with increasing input power (while Type III ELMs are characterised as f_{ELM} decreasing with increasing input power). Other evidence for the ELM type classification as Type I is provided by the size of the individual ELM losses $\Delta W_{ped}/W_{ped}$, $\Delta T_e/T_e$ and $\Delta n_e/n_e$ which are significant and of the order of 10-20% in the ILW database, again typical for Type I ELMs. However, an important difference is a common observation in JET-ILW high triangularity Type I ELMy H-modes that the ELM collapse time scale is much longer than previously observed in JET-C plasmas. In [Loarte-2003] it was reported that the typical 'duration' of the ELM event in JET with the carbon wall is 200ms and was seen in e.g. the pedestal electron temperature collapse. Figure 11a shows the duration of the ELM collapse for a Type I ELMy H-mode in the ILW with I_p/B_t = 2.5MA/2.7T high triangularity (δ~0.42, P_{net} = 15MW) baseline plasma (Pulse No: 82806). The figure shows that the ELM collapse has a long time scale with the initial time scale of the ELM collapse of ~2ms, i.e. ten times longer than the typical time scale observed in JET-C. A subsequent further loss occurs for some of the ELMs with a time scale of 5-10 ms. This secondary collapse is not further discussed here, and is thought to be related to an extended period of reduced confinement. Figure 11b shows a histogram for many individual ELMs in 5 JET-C and 6 JET-ILW high triangularity baseline pulses. Indeed the ELM collapse time is systematically longer for the JET-ILW plasmas. Slow ELMs are potentially good news as they result in reduced peak heat loads to the divertor components. This change in ELM dynamics may be indicative of a change in pedestal stability.

The Peeling Ballooning stability of the pre-ELM pedestal profiles has been determined with the linear MHD stability code MISHKA-1 [Saarelma-NF-2009] for a high triangularly plasma in both JET-C and JET-ILW, Figure 12. The assumptions used for the JET-C and JET-ILW pulse are similar; the T_e and n_e pedestal profiles are obtained from fits to HRTS data in the last 30% of the ELM cycle [e.g. Frassinetti-RSI-2012]. Furthermore, we assume $T_i = T_e$ as the pedestal density is high (6-10 $10^{19}m^{-3}$) and therefore good equipartition between ions and electrons is assured. The impurity profiles in the pedestal are not measured in JET, and therefore the line integrated Z_{eff} measurement is used in the stability analysis and in the calculation of the edge bootstrap current j_{bs} with $<Z_{eff}> = 1.7$ and $<Z_{eff}> = 1.3$ for the JET-C and JET-ILW plasma respectively.

For the JET-C plasma the experimental pre-ELM edge current and pressure gradient j-a point is at the Peeling Ballooning boundary, which is typical for JET Type I ELMy H-mode plasmas [Saarelma-NF-2009, Beurskens-NF-2009, Leyland-NF-submitted, Giroud-NF-2012]. However in

the JET-ILW pulse the Pre-ELM pedestal is 'stable' against the Peeling Ballooning modes. The observations in Figure 12 suggest a difference in edge stability between the two pulses following similar analysis techniques and using data from the same diagnostics. Future work will look into possible effect of increased resistivity because of the reduced pedestal temperatures in JET-ILW high triangularity baseline plasmas as well as the possible role of the edge impurity content.

Unfortunately, we did not obtain sufficiently well resolved pedestal profiles to allow for a linear peeling ballooning stability analysis for all the measured pedestal profiles in the database. Instead we use the EPED model [Snyder-PoP-2009, Snyder-NF-2011], which predicts the pedestal height, and width using calculated peeling-ballooning and kinetic ballooning mode (KBM) constraints. EPED predicts the obtainable pedestal pressure with operational parameters (B_T, I_p, R, a, κ, δ) and plasma physics parameters (global β_N and $n_{e,ped}$) as the input. It uses modelled equilibria with elongation κ and averaged triangularity δ as the input to describe the plasma configuration. For the comparison with EPED, the pre-ELM pedestal pressure must be used. For this large dataset, we use the EPED1 version of the model, which employs a simplified KBM constraint $\Delta_\Psi = 0.076 \sqrt{b_{pol,ped}}$, where the pedestal width Δ_Ψ is defined to be the average of the n_e and T_e widths in normalized poloidal flux. EPED1 couples this KBM constraint with a full (width dependent) calculation of the peeling-ballooning mode stability using the ELITE code on the model equilibria to determine the pressure pedestal width and height self consistently. EPED therefore contains a strong coupling between the pedestal performance and global β, both through its beneficial effect on ballooning stability [Snyder-NF-2007] as well as its indirect beneficial effect, through profile stiffness (Figure 9) on the on the pedestal width.

The ratio of EPED1 predicted to observed pedestal pressure for the all baseline and hybrid JET-C plasmas is 0.97 ± 0.21, with a correlation coefficient of 0.86 between predicted and observed pedestal height [Beurskens-NF-2013]. This standard deviation of 0.21 is in a typical range for studies of EPED model accuracy on several tokamaks [e.g. Groebner-IAEA-2012, Snyder-NF-2009], which typically find agreement within ±20-30%). A comparison of EPED1 predictions to observed pedestal height for both JET-ILW and JET-C cases is shown in Figure 13. For 182 low and 86 high triangularity JET-ILW baseline cases (Figure 13a), the ratio of predicted to observed pedestal pressure is 1.06 ± 0.22, with a correlation coefficient of 0.91. For 64 hybrid cases (Figure 13b), the ratio of predicted to observed pedestal pressure is 1.02 ± 0.15, with a correlation coefficient of 0.76. Note that for the ILW cases, the measured pedestal height is approximated as $2n_{e,ped}\, T_{e,ped}$ (assuming $T_i = T_e$), while for the JET-C cases, the measured total pressure $P_{tot,ped}$ (electron + ion) at the pedestal top location is used.

Figure 13 shows that the EPED predictions for the high triangularity baseline and hybrid plasmas overestimate the actual measured pedestal pressure by an average of 10-20%. Again this observation shows that the influence of triangularity on edge stability has reduced in the JET-ILW. Nevertheless, the reasonable agreement between the measured and EPED1 predicted pedestal pressures shown here indicate that the coupled kinetic ballooning and peeling ballooning model

for the pedestal stability still is a workable model to predict the pedestal parameters in JET-ILW H-modes. However, the model does not explain why the pedestal pressure and confinement is reduced in JET-ILW but shows that if the global pressure is reduced, the edge pedestal is also affected, consistent with the observations in Figure 9.

7. SUMMARY AND CONCLUSIONS

Both the baseline and hybrid Type I ELMy H-mode have been re-established in JET-ILW [Joffrin-IAEA-2012]. For the baseline ELMy H-mode plasmas the normalised global confinement is reduced compared that achieved in JET-C. This reduction in normalised confinement is largely due to the more restricted operational domain where increased gas fuelling is required in order to avoid impurity influxes [Joffrin-IAEA-2012, Puetterich-IAEA-2012]. However a further confinement reduction is observed in the JET-ILW high triangularity baseline plasmas, which is largely due to a lower obtained pedestal temperature [Giroud-IAEA-2012, Beurskens-IAEA-2012]. Similar observations have been made for the JET-ILW hybrid plasmas. For a given fuelling level in both JET-C and JET-ILW the normalised confinement of the hybrid plasmas is comparable for both wall material mixes. However the distribution of pedestal and core confinement has changed in JET-ILW hybrid plasmas; a reduction in the pedestal confinement is compensated by an increased core profile peaking. The reasons for the enhanced profile peaking are still under investigation, and an attempt to obtain an identity match between a JET-ILW and JET-C hybrid plasma [Joffrin-NF-2013] by means of more similar gas fuelling shows a stronger similarity between these two hybrid plasmas, Dedicated experiments in the upcoming JET campaigns will investigate this further.

The confinement in JET-ILW and JET-C has been compared to the ratio $P_{net}/P_{th,08}$ of net input power and the L-H power threshold from the Martin scaling. At low $1< P_{net}/P_{th,08} < 2$ the confinement of the baseline plasmas is significantly reduced in JET-ILW compared to JET-C. After the neutral beam upgrade, which should provide P_{NBI}=35MW, new studies will investigate whether the confinement in the JET-ILW baseline plasmas can be recovered with increased input power and hence increased ratio. The hybrid scenario development has already extended the range up to $P_{net}/P_{th,08} \sim 4$. Here the normalised energy confinement is comparable to that observed in JET-C for similar values of Pnet/Pth08.

Similarly the confinement scaling with net input power shows that the JET-ILW baseline plasmas reside at a lower confinement branch compared to the JET-C plasmas. Nevertheless, a similar confinement degradation is observed between the JET-ILW and JET-C databases which closely follows the international IPB98 scaling $\tau_e \sim P_{net}^{-0.69}$. Comparing plasmas of similar plasmas current ($I_p < 2.1$MA) reveals that in the JET-ILW database a transition can occur from the lower to the higher confinement branch with increasing input power for the hybrid scenario. This effect will be further studied in the upcoming campaigns in dedicated experiments where the confinement properties of both hybrid and baseline plasmas are studied in a systematic scenario comparison experiment, where input power, q_{95} and b are scanned. However this apparent bifurcation indicates

that it is not just input power that determines the normalised confinement. The degradation of the confinement with normalised pressure β_N is much lower in both JET-ILW and JET-C databases combined than is given by the IPB-98 confinement scaling. A linear regression to the current database shows a weak β_N-scaling in energy confinement time τ_e in contrast to the $\tau_{98,2} \sim \beta_N^{-0.9}$ as found in the IPB98 scaling, but confirming the findings in [Luce-PPCF-2008]. Dedicated dimensionless experiments will be conducted in the upcoming campaigns to expose the dimensionless β_N scaling of normalised confinement in JET-ILW. However, if the weak b_N dependence in τ_e holds in JET hybrid and baseline plasmas, it would imply that high b_N operation leads to increased normalised confinement $H_{98(y,2)}$. Due to the limitations in available auxiliary power in ITER, the ITER baseline scenario will operate at low $\beta_N \sim$ 1.5-1.85. For this reason the accessible $H_{98(y,2)}$ vs β_N operational space found in JET baseline plasmas implies $H_{98(y,2)}$~0.8-0.9 for this range of β_N for ITER. Dedicated experiments with nitrogen seeding have shown that the confinement loss in JET-ILW can be largely recovered. These experiments are described in detail in [Giroud-IAEA-2012, Giroud-NF-submitted] and can help towards understanding the reduced confinement with the ILW as well as offer prospects for the recovery of good confinement in the ITER-relevant β_N domain.

As it stands we have no satisfying explanation as to why the changes in wall material have such a great impact on pedestal confinement and why the role of triangularity in edge stability has changed. This is a genuinely unexpected but important result from the JET-ILW experiments. Initial MHD stability analysis shows that the plasmas edge in a JET-ILW high triangularity baseline plasma is seemingly stable with respect to the peeling-ballooning boundary, whereas type I ELM like event still occur. Another indication for the changed edge stability in high triangularity baseline ELMy H-mode plasmas is that the ELM collapse time has increased from typically 200ms in JET-C to ~2ms in JET-ILW. In a wider comparison using the EPED1 model, it seems that the agreement between the model and experiments shows the usual spread of 20-30% in the ratio $p_{ped}/p_{ped,EPED}$. However, there is a separation between the measured and predicted pedestal pressures for low and high triangularity plasmas; the model overpredicts p_{ped} more for high than for low triangularity plasmas. Future experiments will address the detailed role of plasma triangularity in a wider triangularity scan than presented here and will also address the impact of the changed edge impurity content on the pedestal stability.

In Summary, the H-mode experiments in JET-ILW show that the choice of wall material can have a (surprisingly) strong impact on the plasma performance. Projections toward confinement performance in ITER with a Be/W wall may therefore need to be adapted. The database comparison of JET-C and JET-ILW baseline plasmas show that ITER relevant low b_N operation for reference scenario 2 [IPB-NF-98] may lead to a confinement ~20% below the IPB98 scaling in JET-ILW. The ITER hybrid scenario 3 however at $\beta_N > 2.5$ has shown to produce good normalised confinement in JET-ILW matching the requirements with $H_{98(y,2)} > 1$.

ACKNOWLEDGEMENTS

This work, part-funded by the European Communities under the contract of Association between EURATOM/CCFE, was carried out within the framework of the European Fusion Development Agreement. For further information on the contents of this paper please contact publications-officer@jet.efda.org. The views and opinions expressed herein do not necessarily reflect those of the European Commission. This work was also part-funded by the RCUK Energy Programme under grant EP/I501045

REFERENCES

[Beurkens-NF-2009]. M.N.A. Beurskens et al, Nuclear Fusion **49** (2009) 125006

[Beurskens-IAEA-2012]. M.N.A. Beurskens et al, IAEA 2012

[Beurskens-NF-2013]. M.N.A. Beurskens et al., Nuclear Fusion **53** (2013) 013001

[Beurskens-PPCF-2013]. M.N.A. Beurskens et al, submitted to Plasma Physics and Controlled Fusion.

[Brezinsek-PSI-2012]. S. Brezinsek et al, International Conference of Plasma Surface Interaction, Aachen, 2012

[Frassinetti-EPS-2010]. L. Frassinetti et al., 37th EPS Conf. on Plasma Physics, 2010 Dublin, Ireland, P1.1031.

[Frassinetti-EPS-2012]. L. Frassinetti et al., 39th EPS Conf. on Plasma Physics, 2012 Stockholm, Sweden. P4.072

[Frassinetti-RSI-2012]. L. Frassinetti et al. Rev. Sci. Instrum. **83**, 013506 (2012)

[Giroud-NF-2012]. C. Giroud et al, Nuclear Fusion **52** (2012) 063022

[Giroud-IAEA-2012]. C. Giroud et al, IAEA 2012

[Giroud-NF-submitted]. C. Giroud et al, submitted to Nuclear Fusion

[Groebner-IAEA-2012]. R. Groebner, IAEA2012

[Hawryluk-NF-2009]. R.J. Hawryluk et al Nuclear Fusion **49** (2009) 065012 (15pp) doi:10.1088/0029-5515/49/6/065012

[Hobirk-PPCF-2012]. J. Hobirk et al, Plasma Physics and Controlled Fusion **54** (2012) 095001

[Horton-EPS-1999]. L.D. Horton et al., 26th EPS Conf. on Contr. Fusion and Plasma Physics (Maastricht) 1999.

[Huber-PSI-2012]. A. Huber et al, International Conference of Plasma Surface Interaction, Aachen, 2012

[Igitkhanov-CPP-2000]. Igitkhanov Yu and Pogutse O 2000 Contrib. Plasma Physics **40** 368

[IPB-NF-1999]. ITER Physics basis, Nuclear Fusion **39** No 12 (December 1999) 2175-2249

[IPB-NF-2007]. Shimada et al, "progress in the ITER physics basis" - chapter 1, Nuclear Fusion **47** 2007 S1

[Leyland-NF-submitted]. M. Leyland et al. 'Pedestal study in dense high δ ELMy H-mode plasmas

on JET with the Carbon wall' Submitted to Nuclear Fusion
[Lipschultz-PoP-2006]. B. Lipschultz et al, Physics of Plasmas **13**, 056117 2006
[Joffrin-IAEA-2010]. E. Joffrin et al., Proceedings of the 23rd IAEA Fusion Energy Conference, Daejon, Republic of Korea (2010). Paper EX/1-1 http://www-pub.iaea.org/mtcd/meetings/PDFplus/2010/cn180/cn180_papers/exc_1-1.pdf
[Joffrin-IAEA-2012]. E. Joffrin et al, IAEA 2012
[Joffrin-NF-2013]. E. Joffrin et al., submitted to Nuclear Fusion
[Leyland-NF-submitted]. M. Leyland et al, submitted to Nuclear Fusion
[Loarte-PPCF-2003]. A Loarte et al, Plasma Physics and Controlled Fusion (2003) 1549–1569
[Luce-PPCF-2008]. T. Luce et al, Plasma Physics and Controlled Fusion **50** (2008) 043001
[Mantica-PRL-2011]. P. Mantica et al, Physical Review Letters **107**, 135004 (2011)doi:10.1103/PhysRevLett.107.135004
[Martin-JPCS-2008]. Y. Martin et al, JPCS 123 (2008) 012033.
[Matthews-PSI-2012]. International Conference of Plasma Surface Interaction, Aachen, 2012
[Nunes-IAEA-2010]. I Nunes et al., Proceedings of the 23nd IAEA Fusion Energy Conference, Daejon, Republic of Korea (2010).
[Pasqualotto-RSI-2004]. Pasqualotto R. Et al., Review of Scientific Instruments **75**, 3891 (2004)
[Pueterich-IAEA-2012]. T. Pütterich et al., IAEA 2012
[Saarelma-NF-2009]. S. Saarelma et al, Plasma Physics and Controlled Fusion **51** (2009) 035001
[Saarelma-NF-2013]. S. Saarelma et al, Submitted to Nuclear Fusion
[Saibene-NF-1999]. Saibene G et al 1999 Nuclear Fusion **39** 1133
[Saibene-PPCF-2002]. G. Saibene, et al, Plasma Physics and Controlled Fusion **44** (2002) 1769–1799
[Sartori-PPCF-2004]. Sartori R et al. 2004 Plasma Physics and Controlled Fusion **46** 723
[Snyder-NF-2004]. P. Snyder et al, Nuclear Fusion **44** (2004) 320–328
[Snyder-NF-2007]. P. Snyder et al, Nuclear Fusion **47** (2007) 961–968 doi:10.1088/0029-5515/47/8/030
[Snyder-PoP-2009]. P. Snyder et al, Physics of Plasmas **16**, 1 2009
[Snyder-NF-2011]. P. Snyder et al, Nuclear Fusion **51** (2011) 103016
[Schweinzer-NF-2011]. J Schweinzer et al, Nuclear Fusion **51** (2011) 113003 (7pp) doi:10.1088/0029-5515/51/11/113003

Wall	Baseline low δ δ_{av}~0.28	Baseline high δ δ_{av}~0.36-0.45	Hybrid low δ δ_{av}~0.2 (JET-C) δ_{av}~0.25 (JET-ILW)	Hybrid high δ δ_{av}~0.35
Carbon	I_p=1.0-3.0MA q_{95}=2.8-3.5	I_p=1.0-2.5MA q_{95}=3.3-3.6	I_p=1.7-1.9MA q_{95}=3.6-4.0	I_p=1.4-1.9MA q_{95}=3.6-4.5
Be/W	I_p=1.2-3.5MA q_{95}=2.8-4.1	I_p=1.7-2.5MA q_{95}=3.3-3.6	I_p=1.7-2.0MA q_{95}=3.6-4.0	I_p=1.5-1.7MA q_{95}=3.6-4.5

Table 1: Range of current and q_{95} for the ILW and C-wall H-mode database

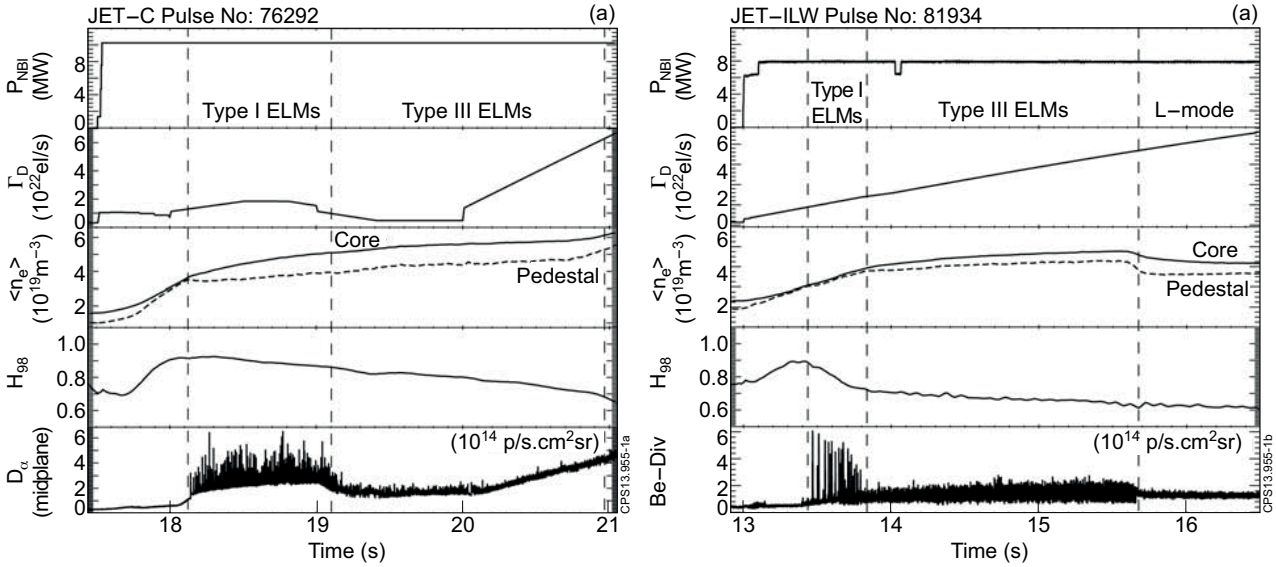

Figure 1: Fuelling ramp in a high triangularity (δ=0.4) ELMy H-mode plasma for a) JET-C at I_p=2MA, B_T=3T, and b) JET-ILW at I_p=2MA, B_T=2.9T. The figures show NBI power P_{NBI}, Deuterium gas fuelling Γ_D, line integrated density $<n_e>$ for core (drawn) and pedestal (dashed), confinement factor $H_{98(y,2)}$ and ELM signature from midplame D_α and divertor Be for JET-C and JET-ILW respectively.

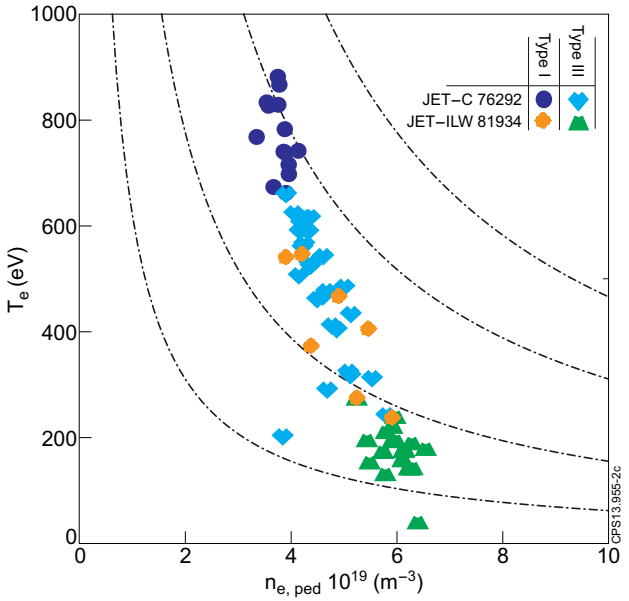

Figure 2: Pedestal electron temperature and density during a density ramp experiment in JET-C and JET-ILW. Blue and red symbols are type I ELMs; cyan and yellow symbols are Type III ELMs. Each dot represents a single time point. The dashed lines represent isobars.

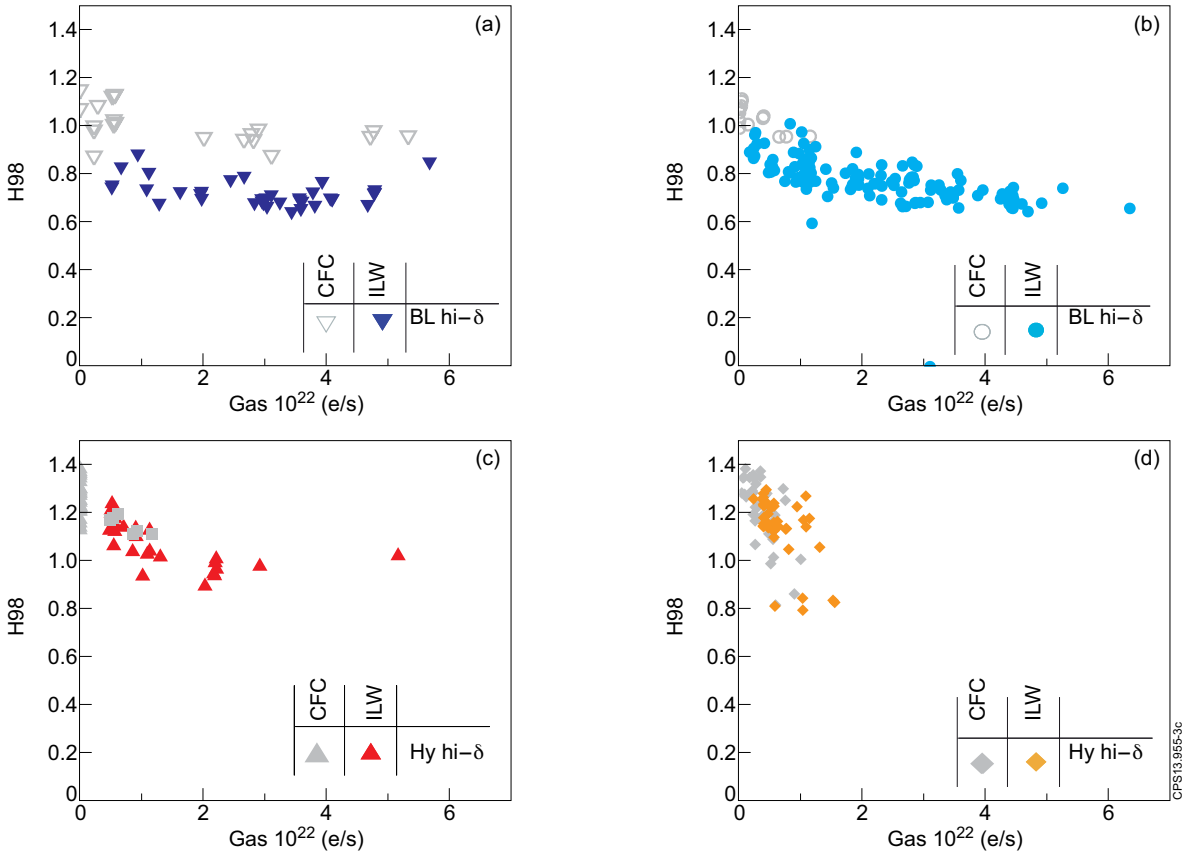

Figure 3: Normalised Confinement enhancement factor as a function of fuelling level for all scenarios. Grey symbols are for JET-C (CFC) plasmas and coloured symbols for JET-ILW (ILW) plasmas. The same colour coding and nomenclature will be used to separate scenarios and wall types in the rest of the paper: a) high triangularity baseline plasmas (BL hi-δ); b) low triangularity baseline plasmas (BL lo-δ); c) high triangularity hybrid plasmas (Hy hi-δ); d) low triangularity baseline plasmas (Hy lo-δ).

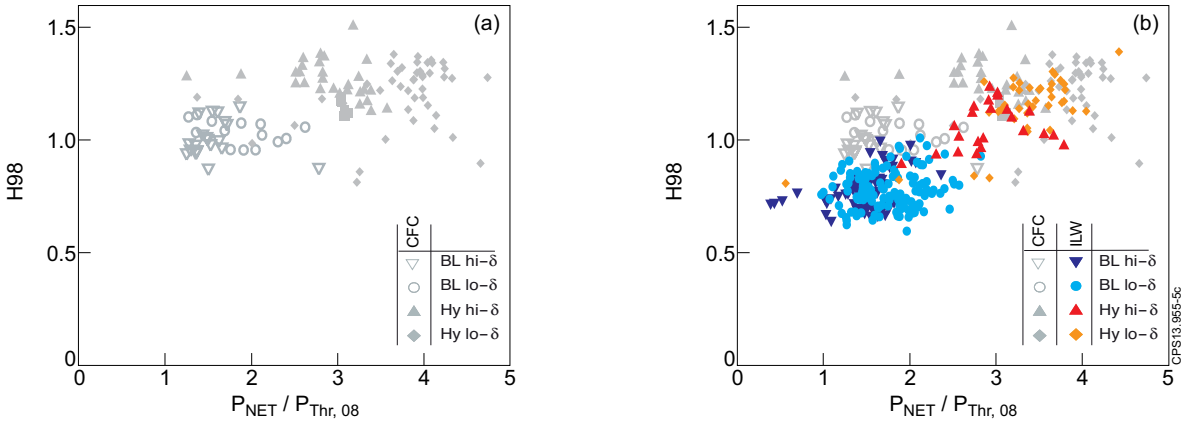

Figure 4: Normalised Confinement enhancement factor as a function of Greenwald density fraction a) for the JET-C plasmas and b) for both JET-C and JET-ILW plasmas.

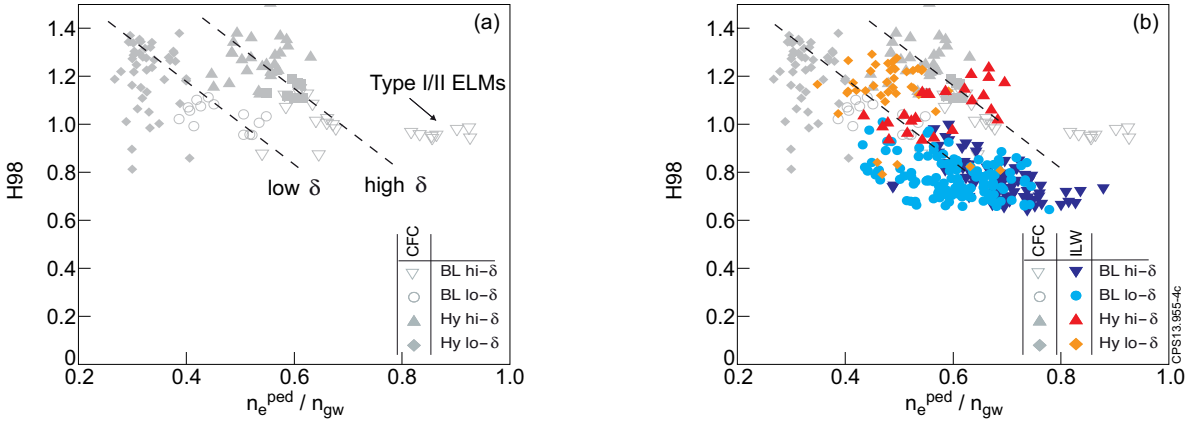

Figure 5: $H_{98(y,2)}$ versus the ratio of $P_{net}/P_{thr,08}$ for (a) JET-C and (b) JET-ILW Hybrid and baseline ELMy H-mode plasmas overlaid.

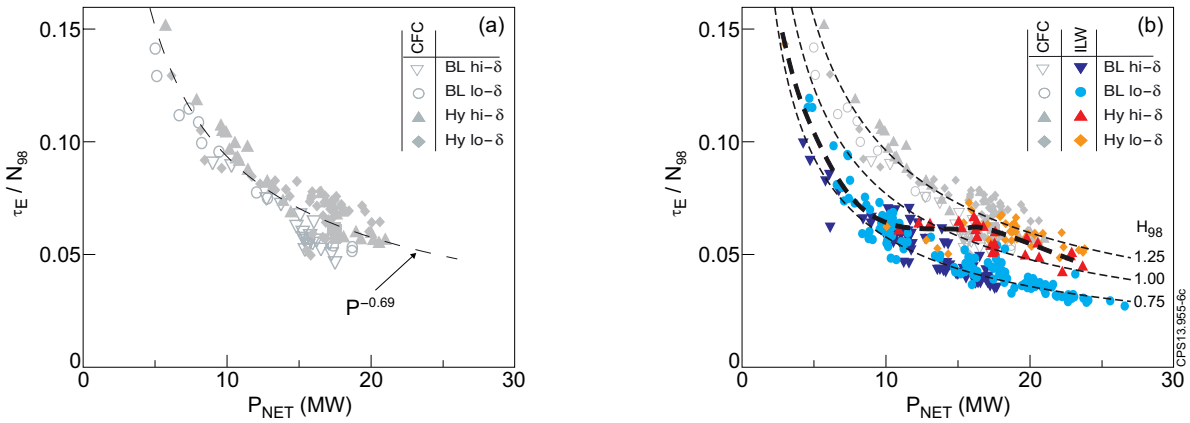

Figure 6: Power degradation of the energy confinement expressed as the measured thermal confinement time normalised to the derived IPB98(y,2)-scaling confinement time $\tau_{98(y,2)}$ excluding the power scaling term $P^{-0.69}$ with $N_{98} = \tau_{98(y,2)}/P^{-0.69} = 0.0562 \times I_p^{0.93} B_t^{0.15} n_e^{0.41} R^{1.39} \kappa^{0.78} a^{0.58} M^{0.19}$ for a) JET hybrid and baseline plasmas in JET-C and b) with JET-ILW data overlaid.

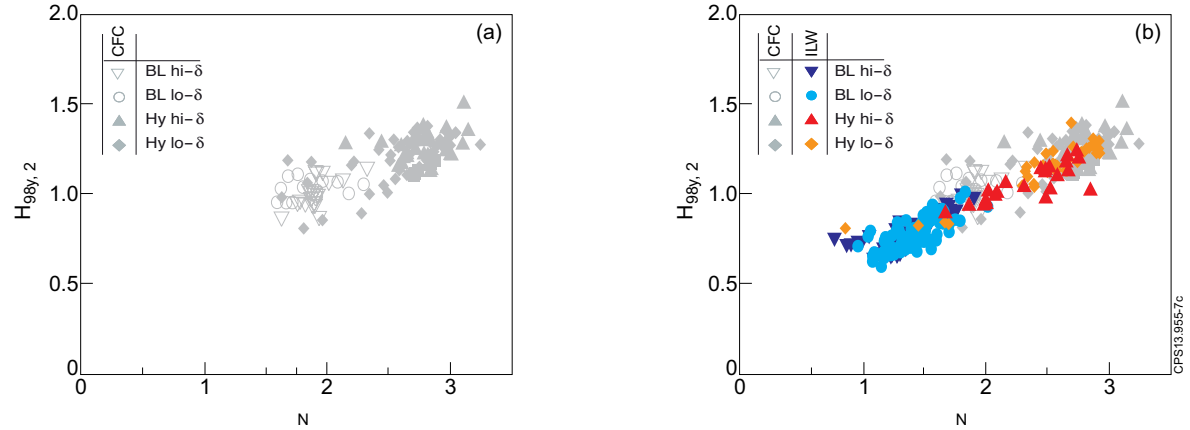

Figure 7: Confinement factor $H_{98(y,2)}$ versus normalised pressure β_N versus for a) JET-C and b) including JET-ILW.

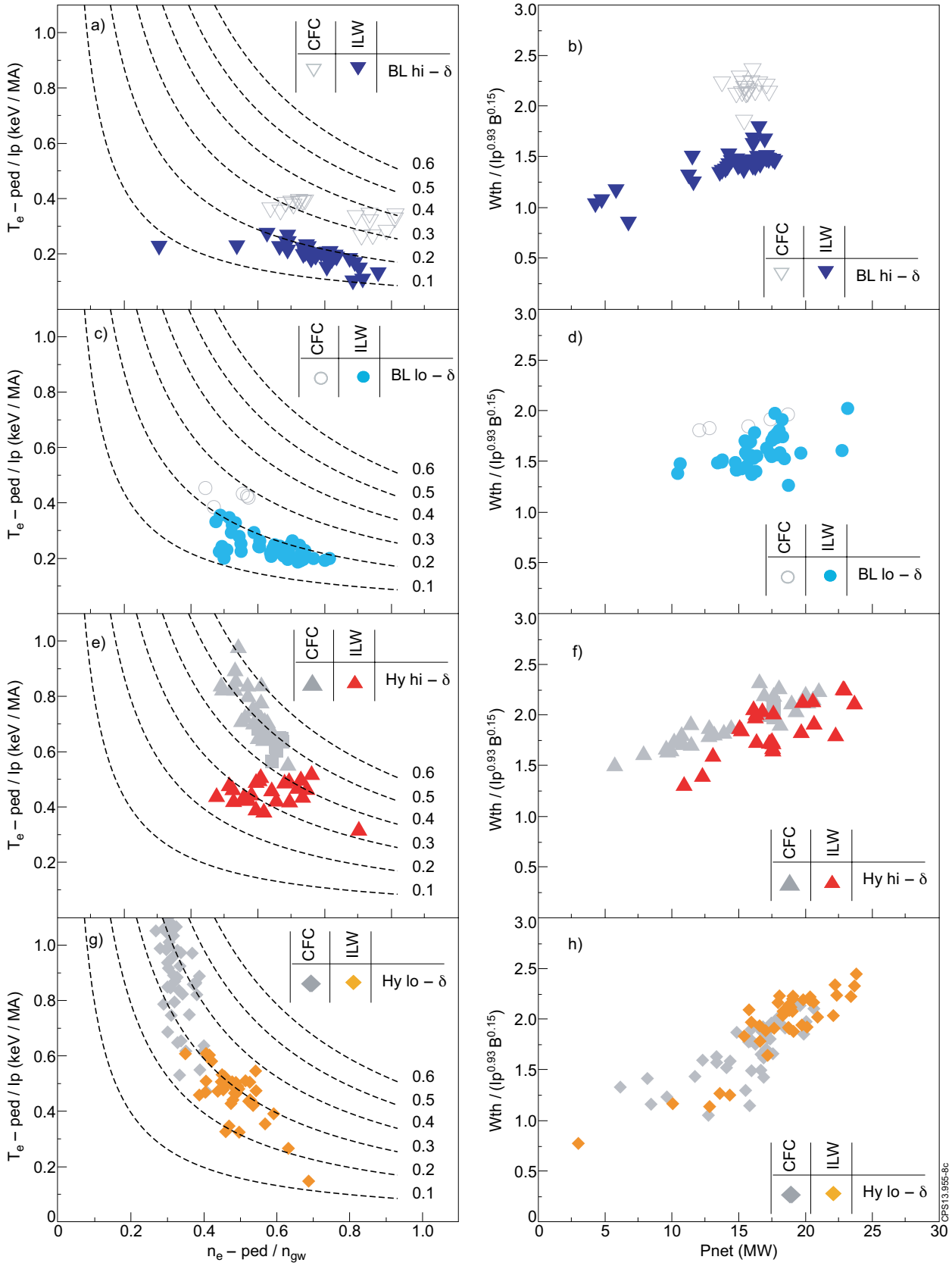

Figure 8: Pedestal T_e and n_e diagram normalised to I_p^2 as T_e/I_p and $n_{e,ped}/n_{gw}$ for JET-C and JET-ILW baseline ELMy H-mode and hybrid plasmas. Thermal stored energy normalised to the IPB-98,y2 scaling the Wth and $I_p^{0.93}$ and $B_t^{0.15}$. for a,b) high triangularity baseline c,d) low triangularity base line plasmas, e,f) high triangularity hybrid plasmas and, g), h) for low triangularity hybrid plasmas.

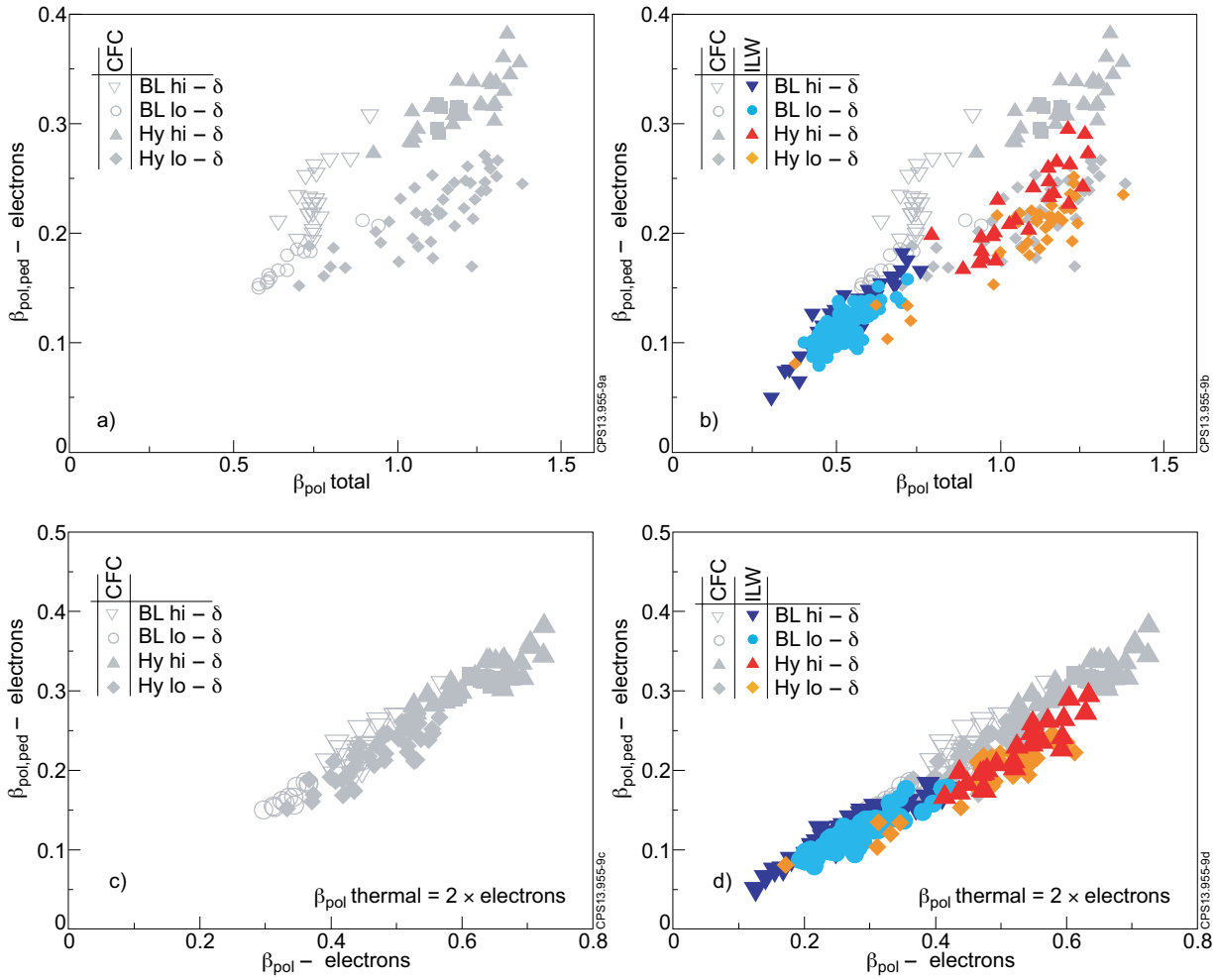

Figure 9: a) Thermal pedestal electron-β_p versus total β_p (from the diamagnetic loop) for JET-C and b) JET-ILW inclusive. The graphs show the role of the total beta on the pedestal stability. c) Thermal pedestal electron-β_p versus thermal electron β_p (from volume integrals of the electron kinetic profiles) for JET-C and d) including the JET-ILW database.

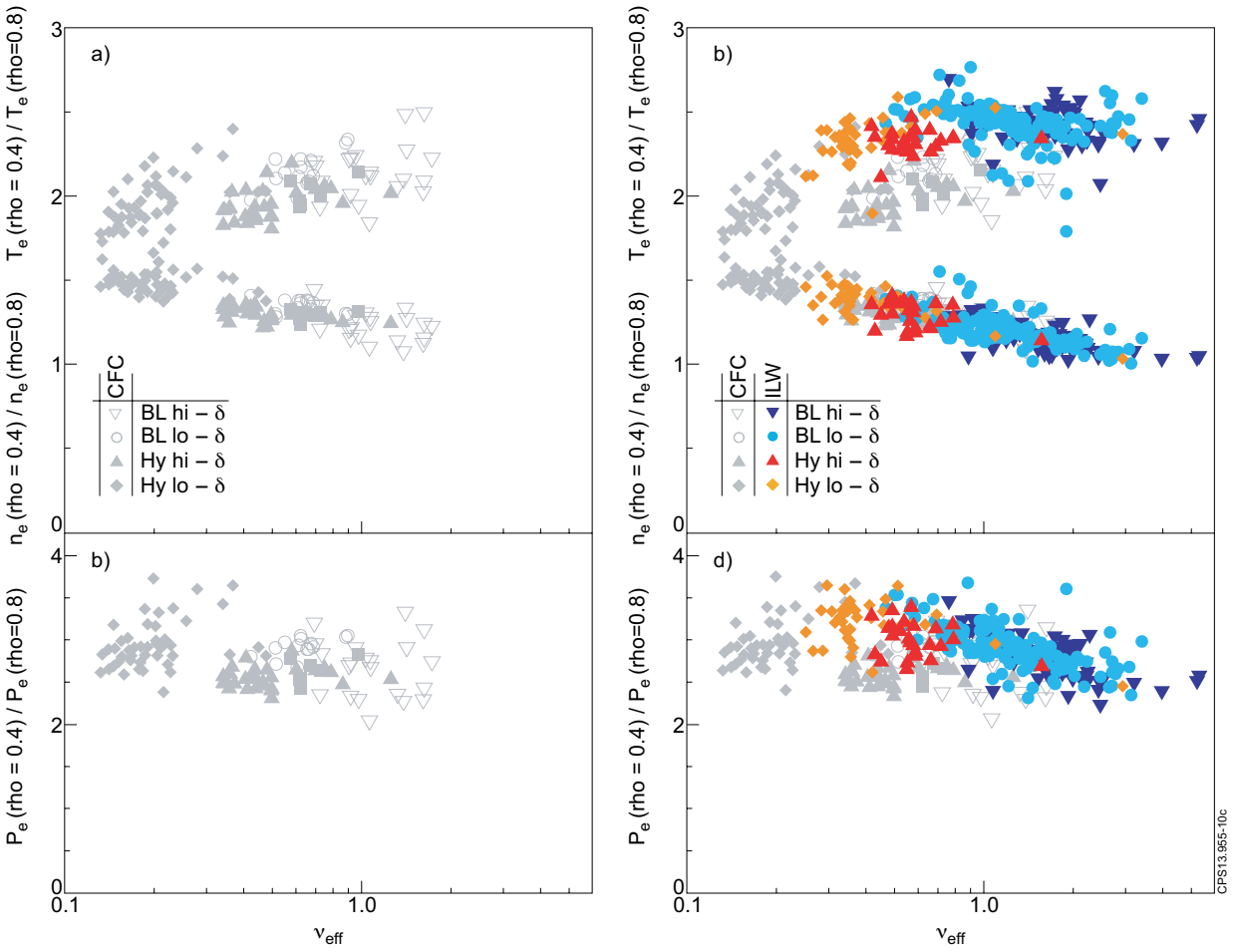

Figure 10: a) and b) Electron temperature and density profile peaking versus collisionality for JET-C and JET-ILW respectively c) and d) electron pressure profile peaking versus collisionality for JET-C and JET-ILW respectively.

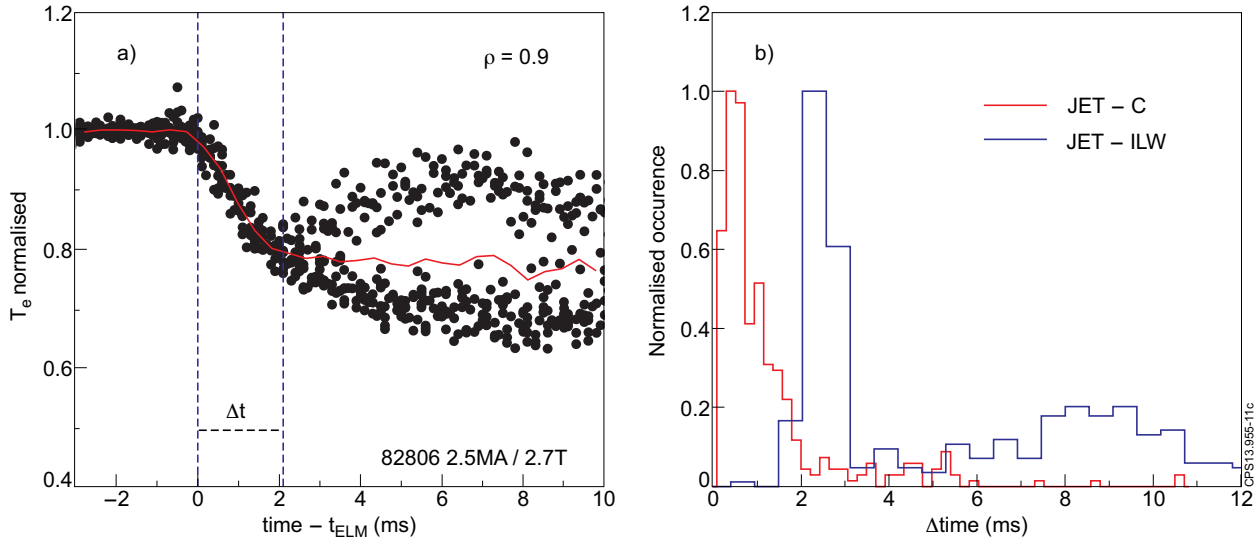

Figure 11: a) ELM collapse time scale for a typical JET-ILW Type I ELMy H-mode with I_p/B_t = 2.5MA/2.7T high triangularity (δ~0.4, P_{net}=15 MW, Γ_D=3x10^{22} el/s) baseline plasma (Pulse No: 82806) b) Histogram of ELM collapse duration from ECE using 5 JET-C and 6 JET-ILW plasmas with I_p/B_t = 2.5MA/2.7T, δ~0.4, P_{net}=14-16 MW, Γ_D=2-4x10^{22} el/s.

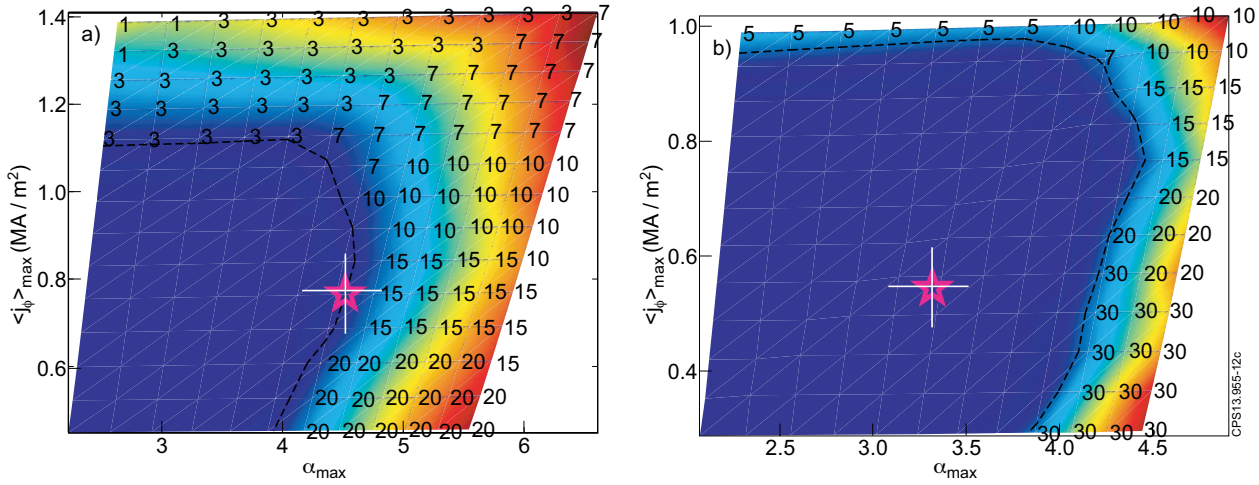

Figure 12: Peeling Ballooning Stability analysis using MISHKA-1 with Tangent hyperbolic fits to HRTS T_e and n_e profiles as an input. for a) JET-C high triangularity plasma (Pulse No: 79503: δ~0.4, P_{net}=15MW, Γ_D=2.5x10^{22} el/s, Z_{eff}=1.7) b) and a JET-ILW plasma (Pulse No: 82806, δ~0.4, P_{net}=15MW, Γ_D=2.5x10^{22} el/s, Z_{eff}=1.3).

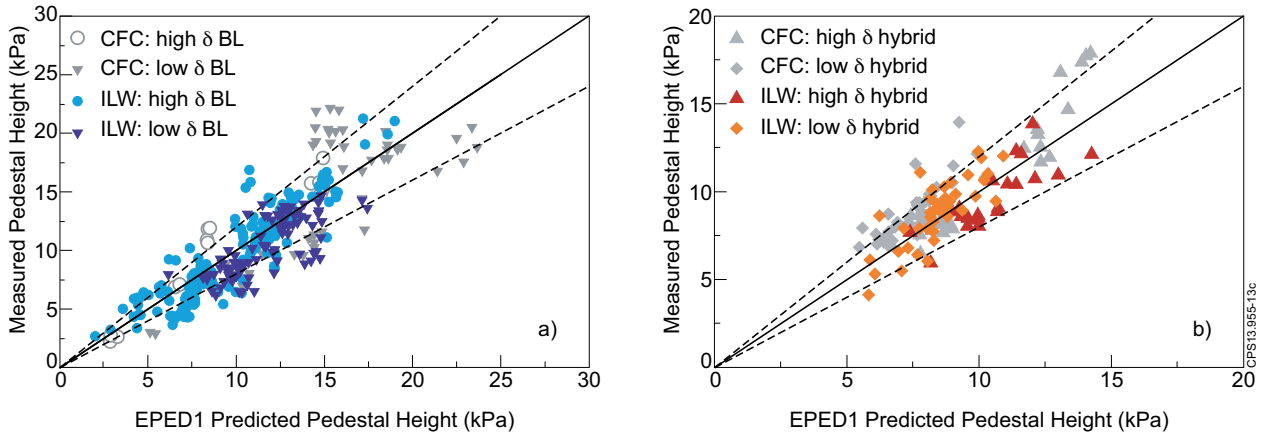

Figure 13: EPED1 predictions for the pedestal height compared to measured values for (a) baseline plasmas and (b) hybrid plasmas for JET-C (grey) and JET-ILW (coloured). The solid line indicates agreement, and the dashed lines ±20%.